Hepatitis B Subviral Envelope Particle Morphogenesis and Intracellular Trafficking

Romuald Patient, Christophe Hourioux, Pierre-Yves Sizaret, Sylvie Trassard, Camille Sureau, Philippe Roingeard

Journal of Virology, April 2007, Vol 81 N° 8, p3842-3851.

Hepatitis B Subviral Envelope Particle Morphogenesis and Intracellular Trafficking

Romuald Patient,[1] Christophe Hourioux,[1] Pierre-Yves Sizaret,[1] Sylvie Trassard,[1] Camille Sureau,[2] and Philippe Roingeard[1]*.

Université François Rabelais, INSERM ERI 19, Tours, France [1], and Laboratoire de Virologie Moléculaire, INTS, Paris, France [2]

Running title : HBs Ag particle morphogenesis and trafficking

* Corresponding author: Philippe Roingeard, INSERM ERI 19 , Laboratoire de Biologie Cellulaire, Faculté de Médecine de Tours, 10 boulevard Tonnellé, F-37032 Tours Cedex France.

Tel (33) 2 47 36 60 71 - Fax (33) 2 47 36 60 90 - E-mail: roingeard@med.univ-tours.fr

ABSTRACT

Hepatitis B virus (HBV) is unusual in that its surface proteins (S, M and L for small, medium and large) are not only incorporated into the virion envelope, but they also bud into empty subviral particles, in great excess over virions. The morphogenesis of these subviral envelope particles remains unclear, but the S protein is essential and sufficient for budding. We show here that in contrast to the presumed model, the HBV subviral particle formed by the S protein self-assembles into branched filaments in the lumen of the endoplasmic reticulum (ER). These long filaments are then folded and bridged for packing into crystal-like structures, which are then transported by ER-derived vesicles to the ER-Golgi intermediate compartment (ERGIC). Within the ERGIC, they are unpacked and relaxed, and their size and shape probably limits further progression through the secretory pathway. Such progression requires their conversion into spherical particles, which occurred spontaneously during the purification of these filaments by affinity chromatography. Small branched filaments are also formed by the L protein in the ER lumen, but these filaments are not packed into transport vesicles. They are transported less efficiently to the ERGIC, potentially accounting for the retention of the L protein within cells. These findings shed light on an important step in the HBV infectious cycle, as the intracellular accumulation of HBV subviral filaments may be directly linked to viral pathogenesis.

INTRODUCTION

The human hepatitis B virus (HBV) is the prototype of the mammalian *Hepadnaviridae* (genus Orthohepadnavirus), a family of small hepatotropic DNA viruses causing acute and chronic liver disease (16). Despite the existence of an effective hepatitis B vaccine, HBV remains a major health problem worldwide, as there is no generally effective treatment for the estimated 350 million chronic carriers who have a high risk of liver cirrhosis and hepatocellular carcinoma. A thorough understanding of HBV morphogenesis and life cycle is thus required for the development of innovative antiviral treatments. The virion (or Dane particle) is a spherical particle, 42 nm in diameter, consisting of an icosahedral nucleocapsid of

approximately 30 nm in diameter and an envelope composed of three surface proteins and, presumably, lipids of host cell origin. The nucleocapsid and envelope are synthesized and mature separately in different cellular compartments, subsequently interacting to form the virion (5, 26, 34). The three HBV envelope proteins are encoded by a single open reading frame (ORF), using three in-frame start codons (21). The large surface protein (L, or p39) is the translation product of the entire ORF (389 to 400 amino acid residues [aa], depending on HBV genotype). The middle surface protein (M, or p30) lacks the N-terminal 119 aa of L (the pre-S1 sequence), and the small surface protein (S, or p24) lacks the N-terminal 55 aa of M (the pre-S2 sequence). These proteins are synthesized at the endoplasmic reticulum (ER) membrane and have a complex transmembrane topology (12, 13). They form disulfide-linked dimers with each other, with no detectable partner preference (27, 45). All three proteins have a form glycosylated at residue N146 in the S domain (gp27, gp33 and gp42 for S, M and L, respectively), but about half the molecules produced remain unglycosylated at this site. The M protein may also be glycosylated (ggp36) at N4 in the pre-S2 domain (17).

HBV and related viruses are unusual among viruses in that the surface proteins are not only incorporated into virion envelopes, they also bud to generate empty subviral spherical or filamentous particles without nucleocapsids in an intracellular compartment, these particles being formed in great excess over virions (21). The S protein is the predominant constituent of these subviral particles and is the essential topogenic element for this budding, with no other viral protein required. Indeed, the production of S protein alone in mammalian cells causes efficient secretion of 20 nm-large subviral particles, also called HBs Ag particles (11, 29). This material is highly immunogenic and is the basis of most vaccines against hepatitis B (14). The type of particle formed seems to be determined by the ratio of S to L proteins coassembling during morphogenesis. The spherical 20 nm HBs Ag particles isolated from the serum of infected patients contain only traces of L protein (21). The coassembly of a higher proportion of L protein with S results in formation of the filamentous form of HBs Ag (21). This high L content inhibits particle secretion (32), due to specific retention motifs in this protein (15, 35) and/or the inefficient export of the filamentous particles (39). The L protein plays a key role in virus assembly and infectivity, and is therefore present in large proportions in the virion envelope (6, 8, 21). The M protein seems to have no determining influence on particle morphology,

because this protein is present in all three particles, in proportions similar to that for S (21). This protein is also dispensable for virion formation *in vitro* (6). It is widely accepted that subviral particles self-assemble at a post-ER/pre-Golgi compartment (ERGIC for ER-Golgi intermediate compartment), together with lipids (24), before their secretion in the constitutive secretory pathway. However, little is known about the molecular mechanisms of the transition of the HBs Ag from the transmembrane to the particulate state, and the intracellular trafficking of this particle.

We have recently shed new light on hepatitis C virus (HCV) morphogenesis, by developing a model based on the production of HCV structural proteins from Semliki Forest Virus (SFV)-derived vectors (1, 2). This model made it possible for the first time to visualize, by electron microscopy (EM), viral assembly and budding at the ER membrane (38). We therefore adopted a similar approach for studies of HBV subviral envelope particle morphogenesis.

MATERIALS AND METHODS

Plasmid construction. The original plasmid pHBV1.5 (generously provided by Dr Volker Bruss), containing an overlength copy of the HBV DNA subtype *adw* (6), was used to extract the sequences encoding the three HBV envelope proteins. We constructed pSFV1-SHBs^{adw} by amplifying a DNA fragment encoding the S protein by PCR from pHBV1.5, using a proofreading *Taq* DNA polymerase (PfuTurbo DNA polymerase, Stratagene) and primers flanked by *Bam*HI restriction endonuclease site sequences (underlined): 5'-Sadw (5' – ATAGGATCC**ATG**GAGAACATCACATCAGGATTCC – 3') and 3'-Sadw (5' – ATAGGATCC**TTATTA**AATGTATACCCAGAGACAAAAGAAAAT – 3'). The start codon and inserted stop codon are indicated in bold typeface. The PCR product was inserted into pGEM®-T (pGEM®-T Easy Vector System, Promega) and then into the *Bam*HI restriction site of the pSFV1 vector (Invitrogen). The plasmids pSFV1-MHBs^{adw} and pSFV1-LHBs^{adw} were obtained in a similar manner, using specific primers flanked by *Xma*I restriction endonuclease site sequences (underlined): 5'-Madw (5' – ATACCCGGG**ATG**CAGTGGAATTCCA – 3') and 5'-Ladw (5' – ATACCCGGG**ATG**GGAGGTTGGTCAT – 3') for the M and L sequences respectively, and 3'-MLadw (5' – ATACCCGGG**TTATTA**AATGTATACCCAGAGACAA – 3') for both M and L

sequences. All PCR products (702 bp, 867 bp and 1224 bp for S, M and L, respectively) were verified by DNA sequencing.

Cell Culture and RNA Transfection. Baby Hamster Kidney cells (BHK-21) were maintained in Glasgow Minimal Essential Medium (Invitrogen) supplemented with 5 % fetal bovine serum (ATGC), 8 % tryptose phosphate (Sigma), 100 IU/mL penicillin and 100 µg/mL streptomycin, in a standard cell incubator, at 37°C under an atmosphere containing 5 % CO_2. For recombinant RNA synthesis, pSFV1 constructs, which contain an SP6 RNA polymerase promoter upstream from the 5' SFV UTR, were linearized at the single *Spe*I site downstream from the multiple cloning site. Linear DNA was transcribed *in vitro,* using SP6 RNA polymerase, according to the standard protocol provided by the manufacturer (Promega). For the negative control, recombinant RNA encoding β-Galactosidase (β-Gal) was synthesized from the pSFV3 expression vector (Invitrogen). BHK-21 cells (10^6) were trypsinized, washed in phosphate-buffered saline (PBS) and mixed with 10 µg of the various recombinant SFV RNAs. They were then electroporated, using a single exponential decay pulse at 350 V, 750 µF in a Gene Pulser Xcell® (Biorad). Immediately after electroporation, cells were diluted in growth medium, plated in a 75 cm^2 culture dish (Falcon) and cultured for 16 hours (unless otherwise specified) before analysis. For confocal microscopy, electroporated cells were cultured directly on 12 mm coverslip in a 24-well plate, at a density of 10^5 cells per coverslip.

Western Blotting. Sixteen hours after transfection, cells were lysed with 1 % NP-40 in Tris-EDTA buffer (1 M Tris pH 8, 1 mM EDTA) supplemented with protein inhibitor cocktail (1 mM phenylmethylsulfonyl, 2 µg/mL aprotinin, 2 µg/mL leupeptin). The lysates were clarified by centrifugation at 4°C for 20 minutes at 12000g. An aliquot of the supernatants was processed for the assessment of protein concentration by the Lowry method. The supernatants were boiled for 5 minutes in disruption buffer (Laemmli buffer containing 5 % β-mercaptoethanol). For western blotting, 10 µg of total proteins were subjected to sodium dodecyl sulfate-polyacrylamide gel electrophoresis (SDS-PAGE) in a 12 % acrylamide gel and transferred to a polyvinylidene difluoride (PVDF) membrane (Hybond P, Amersham). Unsatured sites on the PVDF membranes were blocked with 2 % (wt/vol) non fat milk powder in Tris-buffered saline (TBS) for one hour at room temperature. The membranes were then incubated overnight at 4°C with the rabbit polyclonal antibody

(PAb) anti-HBsAg (R247) (25), diluted 1:2000 in blocking buffer. This antiserum is specific for a linear epitope located between residues 54 and 64 of the S domain (D genotype, aym3 subtype). Membranes were washed with 0.3 % (v/v) Tween in TBS (TBS-T), and incubated for one hour at room temperature with horseradish peroxidase (HRP)-conjugated goat anti-rabbit antibody (Biosource), diluted 1:5000 in blocking buffer. Immunoblots were developed by enhanced chemiluminescence (ECL kit, Amersham) and placed against Kodak Biomax Light films for the detection of light emission.

Confocal Microscopy. Sixteen hours after transfection, cells grown on coverslips were washed in PBS and fixed by incubation with 4 % paraformaldehyde in PBS for 30 minutes at room temperature. Free aldehyde groups were blocked by incubation with 100 mM glycine in PBS for 10 minutes. The cells were then permeabilized by incubation for 30 minutes with 0.05 % saponin, 0.2 % bovine serum albumin (BSA) in PBS. They were then incubated for 30 minutes at room temperature in a dark, humid chamber, with mouse monoclonal antibody (MAb) anti-HBsAg (H25B10, ATCC), rabbit polyclonal antibody (Pab) against calreticulin (anti-CRT, Stressgen) or rabbit PAb against ERGIC53 (Axxora) diluted 1:100, 1:200 and 1:500, respectively, in permeabilization buffer. Cells were washed three times in PBS and incubated with Alexa 488-conjugated goat anti-mouse and Alexa 594-conjugated goat anti-rabbit secondary antibodies (Molecular Probes), diluted 1:2000 and 1:5000, respectively, in permeabilization buffer. Cells were washed three times in PBS and were then mounted in 25 mM Tris pH 8.8, 5 % glycerol, 2.5 % 1,4-diazabicyclo[2,2,2]octane (DABCO) and 10 % polyvinylalcohol MW range 31000-50000 (Sigma). The mounted cells were examined with an Olympus Fluoview 500 confocal laser scanning microscope (Olympus).

Ultrastructural analysis of the transfected cells by EM. Cells were fixed directly in the culture dish 16 hours after electroporation, by incubation for 48 hours in 4 % paraformaldehyde and 1 % glutaraldehyde in 0.1 M phosphate buffer pH 7.2. In some experiments, cells transfected with the pSFV1-SHBs^{adw} construct were subjected to kinetic analysis with fixation 4, 8 and 12 hours after electroporation. Cells were scraped off with a Cell Scraper® (Falcon), washed in PBS, post-fixed for 1 hour with 1 % osmium tetroxide and dehydrated in a graded series of ethanol solutions. Cell pellets were embedded in Epon resin (Sigma), which was allowed to polymerize for 48 hours at 60°C. Ultrathin sections were cut, stained with 5 % uranyl

acetate and 5 % lead citrate, and deposited on EM grids coated with collodion membrane, for examination under a Jeol 1010 transmission electron microscope (TEM). For immuno-EM, transfected BHK-21 cells were fixed by incubation in 4% paraformaldehyde in 0.1 M phosphate buffer (pH 7.2) for 3 h. The cell pellet was then dehydrated in a graded series of ethanol solutions at –20°C, using an automatic freezing substitution system (AFS, Leica), and embedded in London Resin white (Electron Microscopy Science). The resin was allowed to polymerize at –25°C, under UV light, for 72 h. Ultrathin sections were blocked by incubation with 1% fraction V bovine serum albumin (BSA, Sigma) in PBS and incubated with the rabbit PAb against HBs Ag, diluted 1:50 in PBS. Immunolabeling was detected by incubation with gold-conjugated goat anti-rabbit IgG antibodies (British Biocell International) diluted 1:100 in PBS. Ultrathin sections were cut and stained as above and observed with a Jeol 1010 TEM.

HBV subviral envelope particle purification and negative staining by EM. Sixteen hours after transfection, cells were collected from 20 75 cm^2 culture dishes, treated with trypsin, pooled and resuspended in Tris-NaCl buffer (10 mM Tris pH 8, 140 mM NaCl) supplemented with protein inhibitor cocktail (1 mM phenylmethylsulfonyl fluoride, 2 µg/mL aprotinin, 2 µg/mL leupeptin). Cells were lysed by heat shock (2 minutes in liquid nitrogen followed immediately by 2 minutes at 37°C, repeated) and homogenized for 10 minutes on ice. The samples were centrifuged at 4°C, for 15 minutes, at 15000 rpm in an SW41 rotor (Beckman) and the supernatants were concentrated with an Amicon® Ultracell-100k device (Millipore). They were then layered onto the top of a discontinuous sucrose gradient (25 to 60 % in 20 mM Tris pH 8), and centrifuged at 4°C for 16 hours at 28000 rpm in an SW 41 rotor (Beckman). The collected fractions were quantified by immunocapture ELISA, using Maxisorp® plates (Nunc) coated with the mouse anti-HBs MAb H25B10 (ATCC), using the biotinylated mouse anti-HBs MAb H25B10 as a detection reagent. Positive fractions were pooled and dialyzed, using a Slide-A-Lyser® 10000 MWCO dialysis cassette (Pierce Perbio), against 20 mM Tris pH 8 at 4°C, and then concentrated using an Amicon® Ultracell-100k (Millipore) device. This crude preparation (10 µl) was then deposited on EM carbon-coated grids, negatively stained with 1 % uranyl acetate, and analyzed under the TEM. For immunogold labeling, 10 µl of the preparation was first incubated overnight at 4°C with the rabbit

anti-HBs PAb R247, diluted 1:100 in PBS. It was then incubated for 3 hours at room temperature with gold-conjugated goat anti-rabbit IgG antibodies (British Biocell International) diluted 1:50 in PBS. Negative staining was then carried out as described above.

HBV subviral envelope particles were further purified from the initial crude preparation by anti-HBs affinity chromatography. Briefly, the anti-HBs MAb H25B10 was coupled through carbohydrates present in its Fc region, to resin, by mild reduction of the carbohydrate moiety with sodium meta-periodate, followed by covalent coupling to hydrazide gel (CarboLink coupling gel, Pierce). For chromatography, the column was equilibrated with PBS and concentrated samples were loaded onto the column at a flow rate of 1 mL/minute with monitoring of absorbance at 280 nm. Once the samples were loaded, the column was washed with PBS until absorbance reached baseline values. Immunoadsorbed HBsAg particles were eluted with 0.1 M citrate pH 2.9, then collected in 1 mL fractions in tubes containing 0.115 mL of 1 M Tris base, for rapid neutralization of the eluted material. The collected fractions were quantified with the immunocapture ELISA described above. Positive fractions were pooled and dialyzed, using a Slide-A-Lyser® 10000 MWCO dialysis cassette (Pierce Perbio), against 20 mM Tris pH 8 at 4°C. They were then concentrated, using an Amicon® Ultracell-100k (Millipore) device. This final preparation was negatively stained and examined under the TEM as described above.

HBs Ag quantification in the cell supernatants. The amount of HBs Ag present in the supernatant of cells transfected with the various constructs was quantified with the ELISA described above, using sequential dilutions of a recombinant HBs Ag (HBs Ag *adw* R86872, BioDesign) as the standard.

RESULTS

Ultrastructural changes induced by the production of the HBV S envelope protein. Sixteen hours after transfection with the SFV recombinant construct expressing the DNA sequence encoding the HBV S protein, BHK-21 cells were harvested and lysed for western blot analysis (Fig. 1, lane 2). Consistent with previous studies, the S protein was detected in similar quantities of the unglycosylated (p24) and glycosylated (gp27) forms. Confocal microscopy on cells

grown on glass coverslips showed that the S protein colocalized with calreticulin, a specific ER marker, and with the ERGIC marker ERGIC53, mostly in the perinuclear area (Fig. 2, SHBs). Cells transfected with β-Gal RNA gave no signal with anti-HBs antibodies on western blots or on confocal microscopy (Fig. 1 lane 1 and Fig. 2).

Cells producing the S protein displayed significant ultrastructural modifications on EM (Figs. 3 and 4) with respect to the cells producing β-Gal (not shown on figures). Intracellular vesicles, packed with filaments, were abundantly observed in the perinuclear area of these cells (Fig. 3). These vesicles clearly originated from the ER, as they were frequently observed budding from the nuclear envelope (Fig. 3A) or from membranes with ribosomes at their surface (Fig. 3B). They were homogeneous in size (between 0.2 and 0.3 micrometers in diameter) and were filled with packed and presumably bridged filaments, 22-nm in diameter, which were observed in lengthwise or crosswise sections in crystalline structures (Fig. 3C and 3D). The specificity of the content of these vesicles was determined by immunogold labeling with the rabbit PAb against HBs Ag. Modifications to the fixation and embedding procedures required for this specific immunostaining method (particularly the absence of glutaraldehyde and osmium tetroxide), resulted in the cell structures and filaments being less well preserved than in cells embedded in Epon resin according to standard EM methods. However, intense gold labeling restricted to these vesicles was observed in the perinuclear area (inset in Fig. 3D). We carried out a time course analysis and found that these vesicles became detectable as early as 12 hours after transfection, and that their frequency peaked 16 hours after transfection.

We also observed very large cisternae (1 to 2 micrometers in diameter) in some cells. These cisternae were delimited by smooth membranes and contained relaxed long filaments (Fig. 4). Their lumina presumably contained material from the smaller vesicles described above. Indeed, fusion with the cisternae of vesicles containing 22 nm packed filaments was frequently observed (large arrows in Figs. 4B, 4C and 4D). The 22 nm filaments in the lumina of the cisternae were mostly fully relaxed, but in some cases, the filaments were relaxed at one end but remained bridged in a crystalline structure with other filaments at the other (small arrows in Figs. 4A, 4C and 4D). When relaxed, the end of the filament was electron-dense (see the inset in Fig. 4A). These cisternae were observed in cells fixed 16 hours after transfection, but not in cells fixed 4, 8 or 12 hours after transfection.

Negative staining of the intracellular subviral particles formed by the HBV S envelope protein. Initial analysis of the crude cell lysate subjected to centrifugation on a sucrose gradient led to the observation of long filaments 22 nm in diameter (Figs. 5A and 5B). These filaments were well organized, with negative staining revealing a regular crenellated appearance (Fig. 5A and 5B). They were of various sizes, and were often branched (arrows in Fig. 5B). The longest unbranched filament found in this preparation was 1.2 micrometers in length (not shown on the figure). The filaments had bulging extremities, probably accounting for the electron-dense appearance of these extremities in ultrathin sections (see our comment concerning the inset in Fig. 4A above). The specificity of these filaments was confirmed by immunogold labeling. Following prior incubation with the rabbit anti-HBs PAb, the filaments were immunoagglutined and labeled with gold-conjugated goat anti-rabbit IgG antibodies (inset in Fig. 5A). Following purification by affinity chromatography, these filaments were systematically unbranched and much smaller (less than 0.3 micrometers in length), and their ends showed a clear tendency to dissociation into subviral spherical particles (Figs. 5C and 5D).

Ultrastructural changes induced by the production of the HBV M or L envelope proteins. Sixteen hours after transfection with the recombinant SFV constructs containing the DNA sequence of the HBV M or L proteins, BHK-21 cells were harvested and lysed for western blot analysis (Fig. 1). Expression of the pSFV1-MHBs^{adw} construct gave large amounts of glycosylated M protein in cells, with equal amounts of the two main forms (ggp36 and gp33), but only traces of the unglycosylated form (p30). This construct also yielded small amounts of the two forms of the HBV S envelope protein, p24 and gp27 (Fig. 1, lane 3). Expression of the pSFV1-LHBs^{adw} construct yielded large amounts of L protein, with similar amounts of the unglycosylated (p39) and glycosylated (gp42) forms. In contrast to what was observed for pSFV1-MHBs^{adw}, the expression of pSFV1-LHBs^{adw} resulted in the production of only tiny amounts of S proteins. However, expression of this construct yielded two glycosylated forms of M (Fig. 1, lane 4). ELISA showed that HBsAg levels were higher in the supernatant of cells transfected with the pSFV1-MHBs^{adw} construct than in that of cells transfected with the pSFV1-SHBs^{adw} construct (4.6 ng/mL and 1.8 ng/mL, respectively), whereas no HBs Ag was detected in the supernatant of cells transfected with the pSFV1-LHBs^{adw} and β-Gal constructs (Fig. 1). Immunocytochemistry and confocal microscopy showed that the HBV M protein

was partly colocalized with calreticulin and ERGIC53 (Fig. 2), and that the subcellular distribution of this protein was more diffuse than that of the HBV S protein (Fig. 2). The HBV L protein colocalized mostly with calreticulin and, to a lower extend, with ERGIC53, in the perinuclear area of the cells (Fig. 2).

Despite an intensive search and repeated experiments, no ultrastructural changes were detected in cells transfected with the pSFV1-MHBs^{adw} construct (Fig. 6A). In particular, no filamentous or spherical subviral particles were observed in these cells. In contrast, cells transfected with the pSFV1-LHBs^{adw} construct showed dilated convoluted compartments containing filamentous particles (Figs. 6B and 6C). This compartment was probably ER-related, as its membranes were rough and sometimes continuous with the external membrane of the nuclear envelope (Fig. 6B). However, it was much more heterogeneous in size and shape than the ER-related vesicles found in cells producing the HBV S envelope protein. The filaments formed by the HBV L protein also clearly differed from those formed by the HBV S protein: they were slightly larger in diameter, highly branched, unpacked and unbridged (Figs. 6B and 6C). Despite an intensive search, no large cisternae such as those found in cells transfected with the pSFV1-SHBs^{adw} construct were detected in these cells.

Negative staining of intracellular subviral particles formed by the HBV L envelope protein. Analysis of the crude cell lysate subjected to centrifugation on a sucrose gradient revealed the presence of some small, branched filaments with a diameter of 30 nm (Fig. 6D). This observation confirmed that the filaments formed by the HBV L protein differed from those formed by the HBV S protein. They were larger in diameter (30 nm) but much smaller in length (less than 0.5 micrometers). Attempts to purify these filaments further by affinity chromatography were unsuccessful, probably due to their low rate of recovery from the cell lysate and/or their weak binding to the anti-HBs antibody with which the column was coated. We also analyzed a lysate from cells producing the M protein, and confirmed the absence of any filamentous or spherical subviral particles in these cells, at least in sufficient amounts for detection by negative EM staining (data not shown).

DISCUSSION

Despite the existence of hepatoma cell lines that can produce infectious virus after transfection with the viral genome (40, 43) and the recent establishment of a cell

line that can be infected by the virus *in vitro* (20), little is known about the morphogenesis of HBV. This may be due to the low rate of HBV production in these cells, as it has been estimated that an individual hepatocyte releases only 1 to 10 viruses per day during the productive phase of infection *in vivo* (30). HBV subviral envelope particles can reach concentrations 10,000 times higher than that of virions in the serum of infected patients, but their assembly and intracellular transport also remain poorly understood (4).

As the production of the S envelope protein alone is sufficient for the secretion of spherical HBV subviral envelope particles, it is widely thought that the filamentous shape of these particles results from the coproduction of the S and L proteins (7, 21). Our EM study showed that the production of the HBV S protein alone also led, at least initially, to the morphogenesis of filamentous subviral particles. The existence of this phenomenon was suggested in early EM studies on Chinese hamster ovary (CHO) cells producing the HBV S protein (31), but it has not been studied further in the last 20 years. The filaments induced by the HBV S protein in our study seemed to be extremely long (up to 1.2 micrometers) and occasionally branched, a feature that was also considered specific to filaments induced by HBV L protein overproduction in a transgenic mouse model (9).

Our study shows that the morphogenesis of these filaments takes place in the ER. The currently accepted model of the subviral HBV particle formation assumes that this process takes place at the ERGIC membrane, resulting in the budding of the particle into the lumen of this compartment (4). Indeed, biochemical and immunocytochemical studies have suggested that the S protein initially forms dimers, catalyzed by protein disulfide isomerase (PDI) in the ER compartment, before its transport in vesicles, as transmembrane dimers, to the ERGIC (24). The absence of PDI and the presence of different molecules in the lumen of the ERGIC would thus lead to reorganization of the interdimer disulfide bridges, an essential step in the assembly of the subviral particles (24). However, the formation of interdimer disulfide bridges may not be required for particle formation, because most S proteins in particles freshly secreted from transfected cells are dimeric and S mutants with multiple cysteine-to-serine substitutions nonetheless form particles (27, 45). However, direct interactions within S protein subunits are probably required for the formation of subviral envelope particles. Coproduction of the human HBV S protein with its counterpart from an animal hepadnavirus showed that the human and duck

HBV S proteins did not form mixed subviral particles, despite clear structural and sequence similarities, whereas human and woodchuck HBV S, which are more closely related, coassembled efficiently (18). It should also be pointed out that the current model for subviral HBV particle formation is based principally on studies including no ultrastructural analysis of the transfected cells (24). Our EM observations clearly show that the HBV subviral particle formed by the S protein assembles in the ER compartment. Indeed, this phenomenon clearly occurred at ER-related membranes, as the membranes had ribosomes on their surface and/or were continuous with the outer membrane of the nuclear envelope. The HBV subviral particles with a filamentous shape formed by the S protein were initially packed into vesicles budding from the ER, and were then delivered by these vesicles to large cisternae, in which they were unpacked and relaxed. These large cisternae had smooth membranes and probably corresponded to the ERGIC compartment. Unfortunately, it was technically difficult to confirm this hypothesis by immunogold labeling with an anti-ERGIC antibody. The use of Epon resin and standard EM techniques was required to visualize the filaments in this compartment, but the results obtained with anti-ERGIC antibody on ultrathin sections of Epon-embedded cells were unsatisfactory. The HBV subviral filaments formed by the S protein and purified from cell lysates appeared on negative staining to be much longer (up to 1.2 micrometers) than expected from the size of the intracellular vesicles in which they were packed (0.2 to 0.3 micrometers). In addition, these particles were often branched. This indicates that they were probably folded in the vesicles during intracellular trafficking between the ER and the ERGIC. This folding was properly organized, as these packed filaments had a regular, crystal-like structure and were presumably bridged in the vesicles. It has been suggested that chaperones, such as calnexin (36, 44) or BiP (10), are involved in the assembly and morphogenesis of the HBV subviral envelope particles. The ERp57 protein, which is a close homologue of PDI, has also been shown to have chaperone activities in conjunction with calnexin and calreticulin, forming transient mixed disulfide bridges with cellular proteins bearing cysteines (22, 23). These ER-resident proteins may therefore assist with the folding and packing of the HBV subviral envelope filaments during their transport in ER-derived vesicles. The concentrations of these proteins are lower in the ERGIC, which might result in the release of the filaments from these crystal-like structures, as

suggested by our EM observations showing the relaxation of filaments in this compartment.

We were unable to identify the morphological events following the release of the HBV S subviral filaments in the ERGIC. This is not entirely surprising, as the HBV S protein remains in pre-Golgi compartments for almost all of its long lifetime within the cell (31). The high-mannose oligosaccharide chains added to the S protein are converted to the complex form just before secretion, indicating that this protein is rapidly transported to the cell surface through the Golgi apparatus and the final constitutive pathway of vesicular transport (31). It has been suggested that the long half-time of HBV S protein secretion may be accounted for by the rate-limiting step of its assembly into a subviral particle (41). However, we show here that the assembly of the HBV S protein into filamentous particles is an early event, followed by the transport of these filaments towards a compartment probably corresponding to the ERGIC. The rate-limiting step in secretion therefore seems to be the transfer of these particles from the ERGIC to the Golgi apparatus. The filamentous shape of these particles may limit the size of the particles that can be accommodated within transport vesicles. The rate of transport would then be determined by the rate of conversion of a filamentous particle to a more spherical particle. Our observations of HBV S filaments purification by affinity chromatography and the analysis of these filaments by negative staining provide support for this hypothesis, demonstrating that these filaments can be spontaneously converted into spherical particles. Subviral spherical particles purified from the serum of HBV S-transgenic mice were recently reconstructed by cryo-EM, and were found to be very heterogeneous in size (19). This may be due to their formation by dissociation from a precursor filamentous particle. However, it should be noted that extremely long filaments could be transported from the ER to the ERGIC, within small transport vesicles. This may be due to the presence of specific chaperones in the ER compartment, making it possible to fold and to cross-link these long filaments in transport vesicles. In our system, only tiny amounts of HBs Ag were secreted from the transfected cells. This low level of secretion may be accounted for by the high toxicity of the SFV expression system, making it impossible to culture cells for longer than 24 hours, together with the long half-time of HBs Ag secretion. However, HBV subviral particles collected from the supernatant of transfected cells were purified by affinity chromatography and studied by negative staining. Few particles were recovered from

these experiments, but these secreted HBV subviral particles appeared to be spherical, suggesting that the conversion of the filaments to spheres is a prerequisite for their secretion (data not shown). A construct bearing the HBV S gene under the control of the CMV promoter was found to give a ten-fold more efficient HBs Ag secretion than the SFV expression vector, but ultrathin sections of the transfected cells showed no morphological events typical of subviral envelope particle assembly and trafficking. However, the quantification of intracellular HBs Ag by ELISA showed similar amount with the two expression systems (data not shown). The visualisation of the subviral envelope particle assembly with the SFV RNA vectors may be due to a more rapid protein synthesis with this system, leading to a major intracellular accumulation of HBs Ag in the early compartments of the secretory pathway. Also, our efforts to visualise this phenomenon in hepatoma cells such as the Huh7 cell line were unsuccessful, but we have previously observed that the SFV vectors are less efficient in these cells (2).

Many 0.2-0.3 μm vesicles packed with HBV S filaments were seen in the perinuclear area of the cells, but we observed no extrusion of HBV S filaments from the membranes of these vesicles, despite intensive EM analysis of the cells 8, 12 and 16 hours after transfection. Previous studies have shown that the subviral particles contain only 25 % lipid (in terms of weight) (17), so the lipids are unlikely to be organized as in conventional membrane bilayer. The absence of a lipid bilayer in spherical HBV S particles was recently confirmed by cryo-EM analysis (19). Thus, the process resulting in delivery of the HBV S filament to the ER lumen may differ from conventional viral budding. Some EM observations such as those presented in Figs. 3A and 3B suggest that HBV S filaments are assembled *de novo* in the ER lumen, and that a cluster of packaged filaments initiates the budding of a forthcoming transport vesicle. Further investigation is required to confirm or reject this hypothesis.

The production of HBV M and L proteins with an SFV vector had contrasting effects. HBV M protein production did not lead to formation of intracellular filamentous or spherical subviral envelope particles, although the pSFV1-MHBs^{adw} construct also produced the HBV S protein. This lack of particle formation may be accounted for by the much lower level of HBV S protein production induced by the pSFV1-MHBs^{adw} construct than by pSFV1-SHBs^{adw}. However, HBs Ag levels were higher in the supernatant of cells transfected with the pSFV1-MHBs^{adw} construct than in the supernatant of cells transfected with the pSFV1-SHBs^{adw} construct. Confocal

microscopy also showed the subcellular distribution of HBs Ag in the cytoplasma of these cells to be more diffuse. This may reflect a specific role of the M protein in enhancing HBV subviral particle trafficking through the secretory pathway. The M protein is dispensable for virion or subviral envelope particle formation, but an M protein lacking its specific N-linked carbohydrates may inhibit virion (3, 28) or subviral envelope particle (42, 44) secretion. The co-production of a fully glycosylated M with S may therefore promote trafficking of the HBV subviral envelope particles toward the cell surface, as previously suggested (44). Alternatively, we cannot exclude that the HBV M protein could have a specific cytotoxic effect leading to HBs Ag release in the cell supernatant. This phenomenon, together with lower levels of S production, may account for our failure to detect HBV subviral particles in sections of cells transfected with pSFV1-MHBs^{adw}. In contrast, the HBV L protein production led to the morphogenesis of small branched filaments that seemed to accumulate in the lumen of a convoluted, ER-related compartment. Similar ultrastructural observations have been reported with Huh7 hepatoma cells producing HBV L protein alone (46), but our study allowed to compare the morphogenesis of HBV L filaments directly with that of HBV S filaments. Unlike the HBV S filaments, the HBV L filaments were never found packed and bridged in small transport vesicles, and were not targeted to a distal compartment. However, we cannot exclude the possibility that HBV L filaments are transported from the ER to the ERGIC, although if such transport does occur it may be less efficient for these filaments than for HBV S filaments. This hypothesis is supported by the colocalization of HBV L with ERGIC53 on confocal microscopy, which was found to be weaker than that for the HBV S and M proteins. These observations may reflect different affinities of these proteins for the cellular chaperones, which may subsequently contribute to intracellular retention of the HBV L protein.

In conclusion, our study sheds new light on the mechanisms involved in HBV subviral envelope particle morphogenesis and intracellular trafficking through the secretory pathway. As the intracellular accumulation of subviral envelope filaments may be directly linked to the pathogenesis of HBV (9, 33, 37), improvements in our understanding of these mechanisms might facilitate the design of new antiviral strategies in future studies.

ACKNOWLEDGMENTS

We would like to thank Dr Didier Leturcq, R.W. Johnson Pharmaceutical Research Institute in San Diego, for his invaluable help in setting up the affinity chromatography system. We thank Dr Volker Bruss, University of Göttingen, for the gift of the pHBV1.5 plasmid. Our research is supported by the *Region Centre (Equipe ESPRI)*, and ANRS. R.P. was supported by a fellowship from the French Ministry of Research. Our data were generated with the help of the RIO Electron Microscopy Facility of François Rabelais University.

REFERENCES

1. **Blanchard, E., D. Brand, S. Trassard, A. Goudeau, and P. Roingeard.** 2002. Hepatitis C virus-like particle morphogenesis. J Virol **76:**4073-9.
2. **Blanchard, E., C. Hourioux, D. Brand, M. Ait-Goughoulte, A. Moreau, S. Trassard, P. Y. Sizaret, F. Dubois, and P. Roingeard.** 2003. Hepatitis C virus-like particle budding: role of the core protein and importance of its Asp111. J Virol **77:**10131-8.
3. **Block, T. M., X. Lu, A. Mehta, J. Park, B. S. Blumberg, and R. Dwek.** 1998. Role of glycan processing in hepatitis B virus envelope protein trafficking. Adv Exp Med Biol **435:**207-16.
4. **Bruss, V.** 2004. Envelopment of the hepatitis B virus nucleocapsid. Virus Res **106:**199-209.
5. **Bruss, V.** 1997. A short linear sequence in the pre-S domain of the large hepatitis B virus envelope protein required for virion formation. J Virol **71:**9350-7.
6. **Bruss, V., and D. Ganem.** 1991. The role of envelope proteins in hepatitis B virus assembly. Proc Natl Acad Sci U S A **88:**1059-63.
7. **Bruss, V., E. Gerhardt, K. Vieluf, and G. Wunderlich.** 1996. Functions of the large hepatitis B virus surface protein in viral particle morphogenesis. Intervirology **39:**23-31.
8. **Bruss, V., and K. Vieluf.** 1995. Functions of the internal pre-S domain of the large surface protein in hepatitis B virus particle morphogenesis. J Virol **69:**6652-7.
9. **Chisari, F. V., P. Filippi, J. Buras, A. McLachlan, H. Popper, C. A. Pinkert, R. D. Palmiter, and R. L. Brinster.** 1987. Structural and pathological effects of synthesis

of hepatitis B virus large envelope polypeptide in transgenic mice. Proc Natl Acad Sci U S A **84:**6909-13.

10. **Cho, D. Y., G. H. Yang, C. J. Ryu, and H. J. Hong.** 2003. Molecular chaperone GRP78/BiP interacts with the large surface protein of hepatitis B virus in vitro and in vivo. J Virol **77:**2784-8.
11. **Dubois, M. F., C. Pourcel, S. Rousset, C. Chany, and P. Tiollais.** 1980. Excretion of hepatitis B surface antigen particles from mouse cells transformed with cloned viral DNA. Proc Natl Acad Sci U S A **77:**4549-53.
12. **Eble, B. E., V. R. Lingappa, and D. Ganem.** 1986. Hepatitis B surface antigen: an unusual secreted protein initially synthesized as a transmembrane polypeptide. Mol Cell Biol **6:**1454-63.
13. **Eble, B. E., V. R. Lingappa, and D. Ganem.** 1990. The N-terminal (pre-S2) domain of a hepatitis B virus surface glycoprotein is translocated across membranes by downstream signal sequences. J Virol **64:**1414-9.
14. **Eddleston, A.** 1990. Modern vaccines. Hepatitis. Lancet **335:**1142-5.
15. **Gallina, A., E. Gazina, and G. Milanesi.** 1995. A C-terminal PreS1 sequence is sufficient to retain hepatitis B virus L protein in 293 cells. Virology **213:**57-69.
16. **Ganem, D., and A. M. Prince.** 2004. Hepatitis B virus infection--natural history and clinical consequences. N Engl J Med **350:**1118-29.
17. **Gavilanes, F., J. M. Gonzalez-Ros, and D. L. Peterson.** 1982. Structure of hepatitis B surface antigen. Characterization of the lipid components and their association with the viral proteins. J Biol Chem **257:**7770-7.
18. **Gerhardt, E., and V. Bruss.** 1995. Phenotypic mixing of rodent but not avian hepadnavirus surface proteins into human hepatitis B virus particles. J Virol **69:**1201-8.
19. **Gilbert, R. J., L. Beales, D. Blond, M. N. Simon, B. Y. Lin, F. V. Chisari, D. I. Stuart, and D. J. Rowlands.** 2005. Hepatitis B small surface antigen particles are octahedral. Proc Natl Acad Sci U S A **102:**14783-8.
20. **Gripon, P., S. Rumin, S. Urban, J. Le Seyec, D. Glaise, I. Cannie, C. Guyomard, J. Lucas, C. Trepo, and C. Guguen-Guillouzo.** 2002. Infection of a human hepatoma cell line by hepatitis B virus. Proc Natl Acad Sci U S A **99:**15655-60.
21. **Heermann, K. H., U. Goldmann, W. Schwartz, T. Seyffarth, H. Baumgarten, and W. H. Gerlich.** 1984. Large surface proteins of hepatitis B virus containing the pre-s sequence. J Virol **52:**396-402.

22. **Helenius, A., and M. Aebi.** 2001. Intracellular functions of N-linked glycans. Science **291:**2364-9.

23. **Helenius, A., and M. Aebi.** 2004. Roles of N-linked glycans in the endoplasmic reticulum. Annu Rev Biochem **73:**1019-49.

24. **Huovila, A. P., A. M. Eder, and S. D. Fuller.** 1992. Hepatitis B surface antigen assembles in a post-ER, pre-Golgi compartment. J Cell Biol **118:**1305-20.

25. **Jenna, S., and C. Sureau.** 1999. Mutations in the carboxyl-terminal domain of the small hepatitis B virus envelope protein impair the assembly of hepatitis delta virus particles. J Virol **73:**3351-8.

26. **Le Pogam, S., and C. Shih.** 2002. Influence of a putative intermolecular interaction between core and the pre-S1 domain of the large envelope protein on hepatitis B virus secretion. J Virol **76:**6510-7.

27. **Mangold, C. M., F. Unckell, M. Werr, and R. E. Streeck.** 1995. Secretion and antigenicity of hepatitis B virus small envelope proteins lacking cysteines in the major antigenic region. Virology **211:**535-43.

28. **Mehta, A., X. Lu, T. M. Block, B. S. Blumberg, and R. A. Dwek.** 1997. Hepatitis B virus (HBV) envelope glycoproteins vary drastically in their sensitivity to glycan processing: evidence that alteration of a single N-linked glycosylation site can regulate HBV secretion. Proc Natl Acad Sci U S A **94:**1822-7.

29. **Moriarty, A. M., B. H. Hoyer, J. W. Shih, J. L. Gerin, and D. H. Hamer.** 1981. Expression of the hepatitis B virus surface antigen gene in cell culture by using a simian virus 40 vector. Proc Natl Acad Sci U S A **78:**2606-10.

30. **Nowak, M. A., S. Bonhoeffer, A. M. Hill, R. Boehme, H. C. Thomas, and H. McDade.** 1996. Viral dynamics in hepatitis B virus infection. Proc Natl Acad Sci U S A **93:**4398-402.

31. **Patzer, E. J., G. R. Nakamura, C. C. Simonsen, A. D. Levinson, and R. Brands.** 1986. Intracellular assembly and packaging of hepatitis B surface antigen particles occur in the endoplasmic reticulum. J Virol **58:**884-92.

32. **Persing, D. H., H. E. Varmus, and D. Ganem.** 1986. Inhibition of secretion of hepatitis B surface antigen by a related presurface polypeptide. Science **234:**1388-91.

33. **Phillips, M. J., R. Cameron, M. A. Flowers, L. M. Blendis, P. D. Greig, I. Wanless, M. Sherman, R. Superina, B. Langer, and G. A. Levy.** 1992. Post-transplant recurrent hepatitis B viral liver disease. Viral-burden, steatoviral, and fibroviral hepatitis B. Am J Pathol **140:**1295-308.

34. **Poisson, F., A. Severac, C. Hourioux, A. Goudeau, and P. Roingeard.** 1997. Both pre-S1 and S domains of hepatitis B virus envelope proteins interact with the core particle. Virology **228:**115-20.

35. **Prange, R., A. Clemen, and R. E. Streeck.** 1991. Myristylation is involved in intracellular retention of hepatitis B virus envelope proteins. J Virol **65:**3919-23.

36. **Prange, R., M. Werr, and H. Loffler-Mary.** 1999. Chaperones involved in hepatitis B virus morphogenesis. Biol Chem **380:**305-14.

37. **Roingeard, P.** 2003. Vacuolization in hepatitis B virus-infected hepatocytes. Hepatology **37:**1223-4.

38. **Roingeard, P., C. Hourioux, E. Blanchard, D. Brand, and M. Ait-Goughoulte.** 2004. Hepatitis C virus ultrastructure and morphogenesis. Biol Cell **96:**103-8.

39. **Roingeard, P., and C. Sureau.** 1998. Ultrastructural analysis of hepatitis B virus in HepG2-transfected cells with special emphasis on subviral filament morphogenesis. Hepatology **28:**1128-33.

40. **Sells, M. A., M. L. Chen, and G. Acs.** 1987. Production of hepatitis B virus particles in Hep G2 cells transfected with cloned hepatitis B virus DNA. Proc Natl Acad Sci U S A **84:**1005-9.

41. **Simon, K., V. R. Lingappa, and D. Ganem.** 1988. Secreted hepatitis B surface antigen polypeptides are derived from a transmembrane precursor. J Cell Biol **107:**2163-8.

42. **Sureau, C., C. Fournier-Wirth, and P. Maurel.** 2003. Role of N glycosylation of hepatitis B virus envelope proteins in morphogenesis and infectivity of hepatitis delta virus. J Virol **77:**5519-23.

43. **Sureau, C., J. L. Romet-Lemonne, J. I. Mullins, and M. Essex.** 1986. Production of hepatitis B virus by a differentiated human hepatoma cell line after transfection with cloned circular HBV DNA. Cell **47:**37-47.

44. **Werr, M., and R. Prange.** 1998. Role for calnexin and N-linked glycosylation in the assembly and secretion of hepatitis B virus middle envelope protein particles. J Virol **72:**778-82.

45. **Wunderlich, G., and V. Bruss.** 1996. Characterization of early hepatitis B virus surface protein oligomers. Arch Virol **141:**1191-205.

46. **Xu, Z., V. Bruss, and T. S. Yen.** 1997. Formation of intracellular particles by hepatitis B virus large surface protein. J Virol **71:**5487-94.

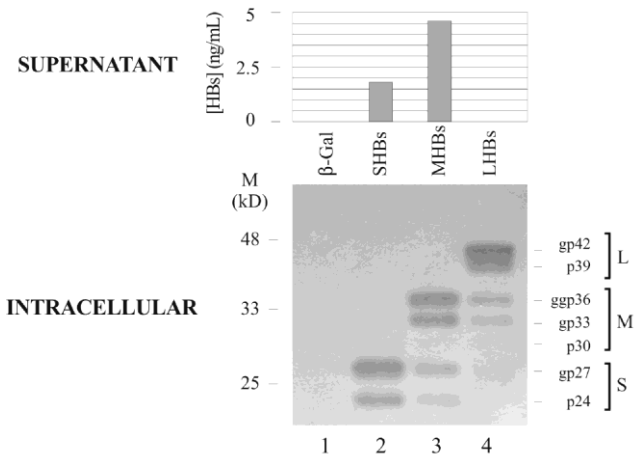

FIG. 1. Analysis of HBV envelope protein production in BHK-21 cells transfected with pSFV1-SHBs^{adw}, pSFV1-MHBs^{adw} or pSFV1-LHBs^{adw}. Western blots showed that the transfection with the pSFV1-SHBs^{adw} construct led to the production of S protein in large amounts, with equal proportions of the unglycosylated (p24) and glycosylated (gp27) forms. Transfection with pSFV1-MHBs^{adw} led to the production within cells of the two main forms of the glycosylated M protein (ggp36 and gp33) but only trace amounts of the unglycosylated form (p30), with small amounts of the two forms of the HBV S envelope protein, p24 and gp27. Transfection with pSFV1-LHBs^{adw} led to the production of the L protein in its unglycosylated (p39) and glycosylated (gp42) forms, and to the production of smaller amount of the two glycosylated forms of M. ELISA showed that HBsAg levels were twice as high in the supernatant of cells transfected with pSFV1-MHBs^{adw} than in the supernatant of cells transfected with pSFV1-SHBs^{adw}, and that no HBs Ag was present in the supernatant of cells transfectd with the pSFV1-LHBs^{adw} and β-Gal constructs. Molecular weight markers (M) are indicated on the left of the blot.

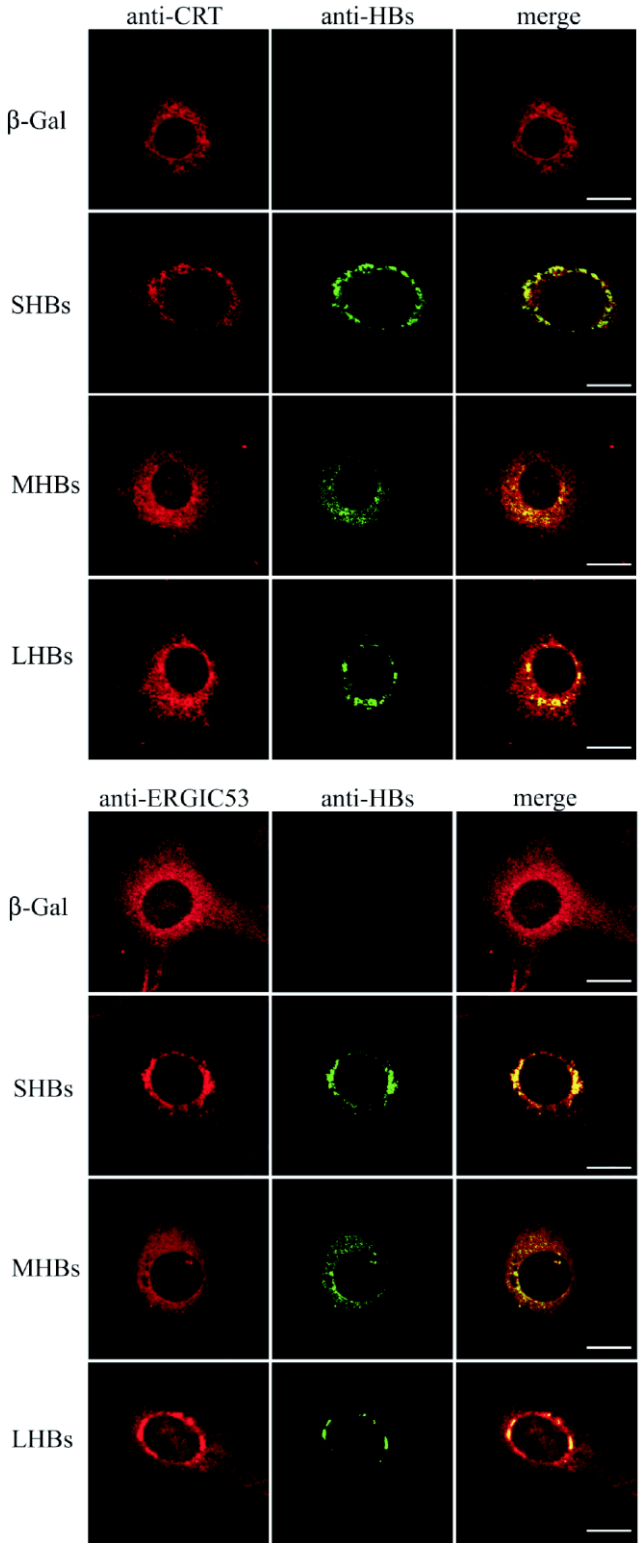

FIG. 2. Subcellular localization, by confocal microscopy, of the HBV envelope proteins in BHK-21 cells transfected with pSFV1-SHBs^{adw}, pSFV1-MHBs^{adw} or pSFV1-LHBs^{adw}. All three proteins colocalized at least partly with calreticulin, a specific ER marker, and with ERGIC53, a specific ERGIC marker, in the perinuclear area. The HBV M protein had a more diffuse subcellular distribution than the S and L proteins. The HBV L protein was found mostly colocalized with calreticulin and, to a lesser extend, with ERGIC53. Cells transfected with a recombinant SFV RNA encoding the β-Gal were used as a negative control.

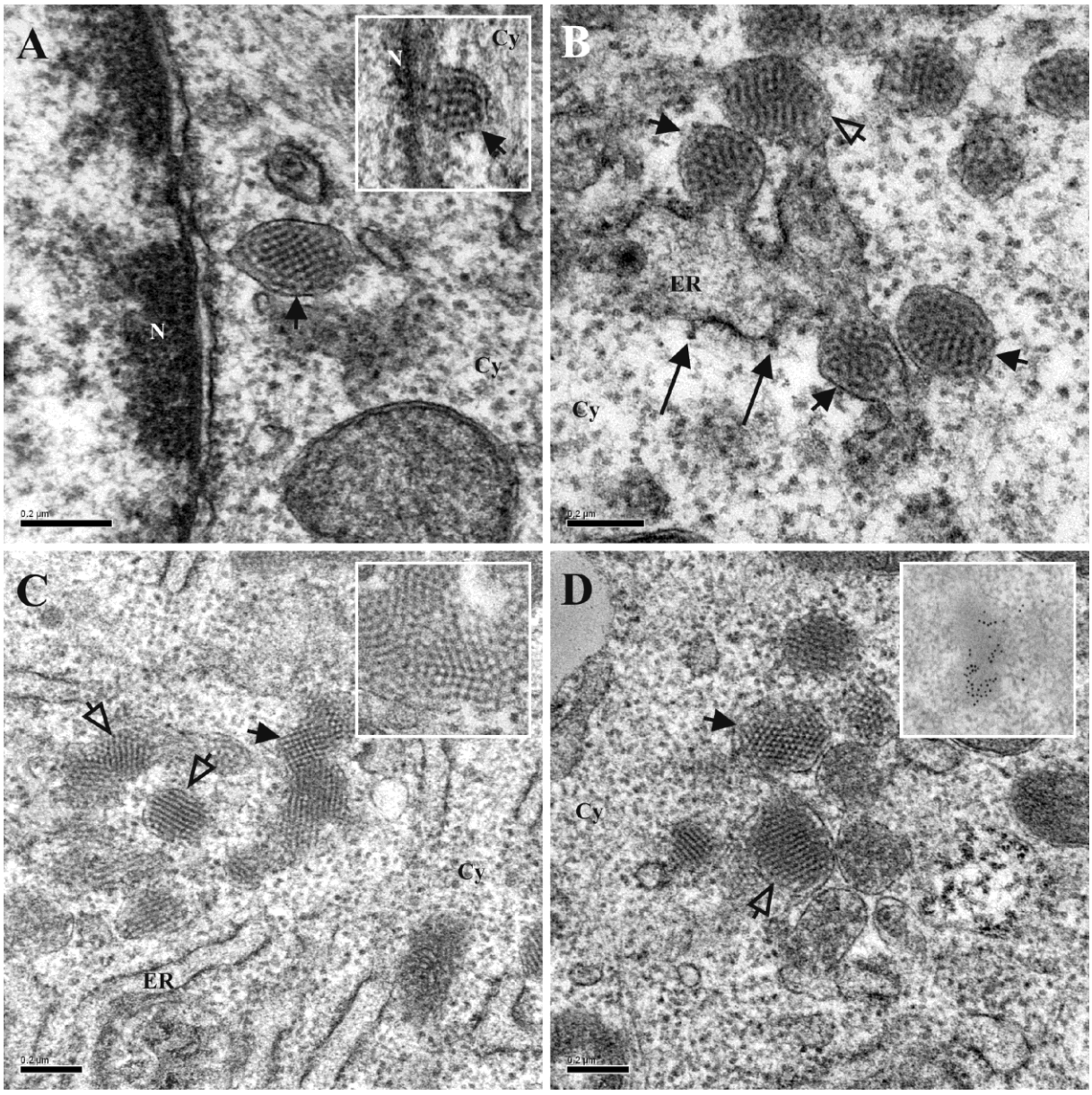

FIG. 3. Early ultrastructural changes in BHK-21 cells producing the HBV S protein. Numerous vesicles 0.2 to 0.3 μm in diameter (short arrows), packed with 22 nm large filaments, were observed in the perinuclear area. These vesicles originated from the ER, as they were frequently observed budding from the nuclear envelope (A and its inset) or from membranes carrying ribosomes (indicated by the long arrows in B). The filaments packed in these vesicles appeared in lengthwise (open arrows) or crosswise (closed arrows) sections in crystal-like structures (see a high magnification of these packed filaments in the inset in C). The specificity of these filaments was studied by immuno-EM using the rabbit anti-HBs PAb. Modifications to the fixation and embedding procedures required for this specific immunostaining method, resulted in cell structures and filaments being less well preserved than in cells embedded in Epon resin and subjected to standard EM procedures, but intense gold labeling restricted to these vesicles and predominantly found in the perinuclear area was observed (inset in D). No specific ultrastructural changes were observed in cells producing β-Gal (not shown on figures). Bars, 0.2 micrometers; N, nucleus; ER, endoplasmic reticulum ; Cy, cytoplasma.

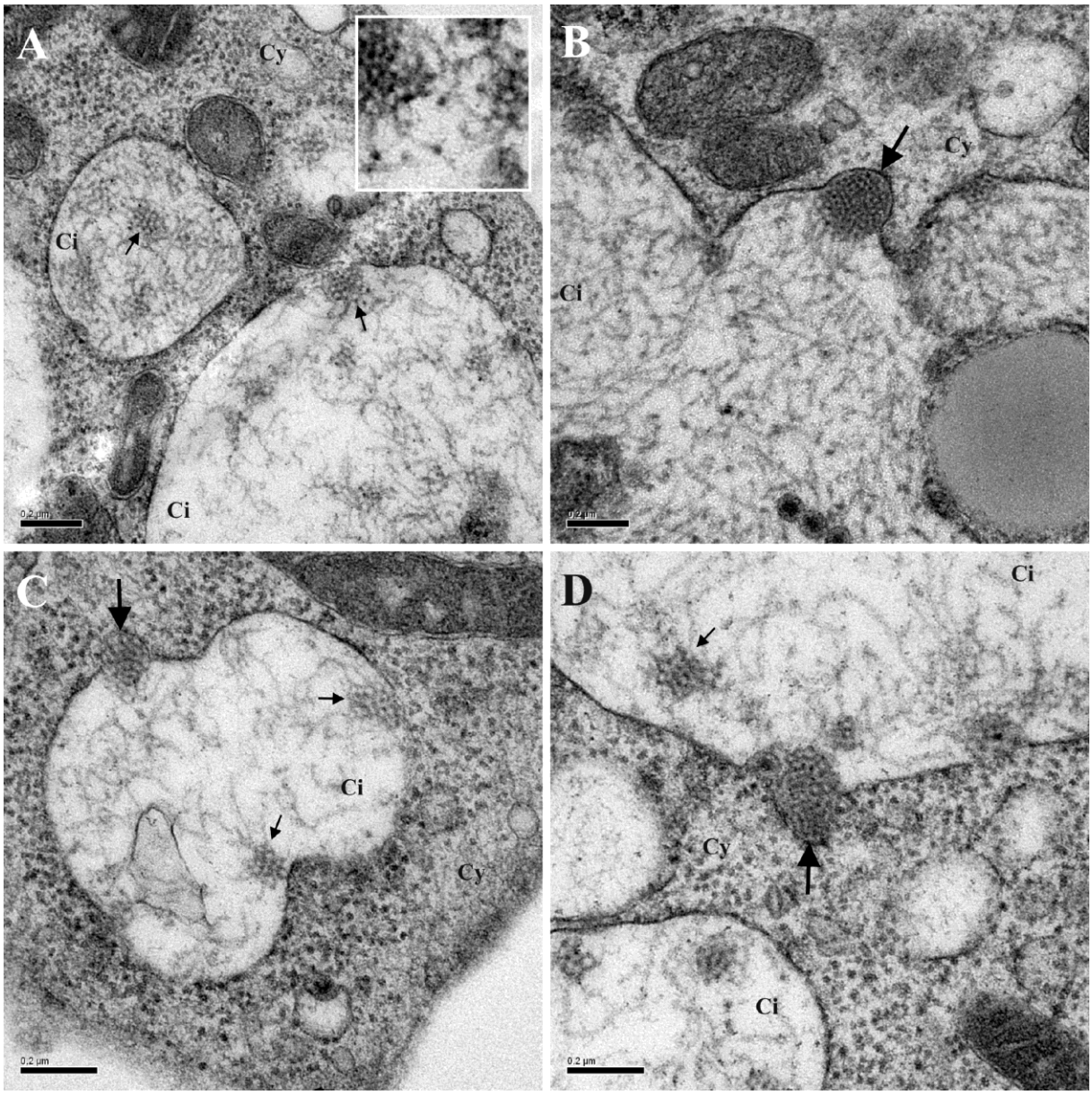

FIG. 4. Late ultrastructural changes in BHK-21 cells producing the HBV S protein. Very large cisternae with smooth membranes, 1 to 2 micrometers in diameter, were found to contain interlaced relaxed 22 nm diameter filaments (A). The ends of these filaments appeared electron-dense (see a high magnification of these filaments in the inset in A). The fusion of vesicles transporting packed filaments with the membranes of cisternae was frequently observed (large arrows in B, C and D), suggesting that the lumina of these cisternae contained material provided by the vesicles with the packed filaments. Filaments in the lumen were sometimes relaxed to one end, with the other end remaining associated with a cristal-like structure and other filaments (small arrows in A, C and D). These ultrastructural changes were never observed in cells producing β-Gal (not shown on figures). Bars, 0.2 micrometers; Ci, cisterna; Cy, cytoplasma.

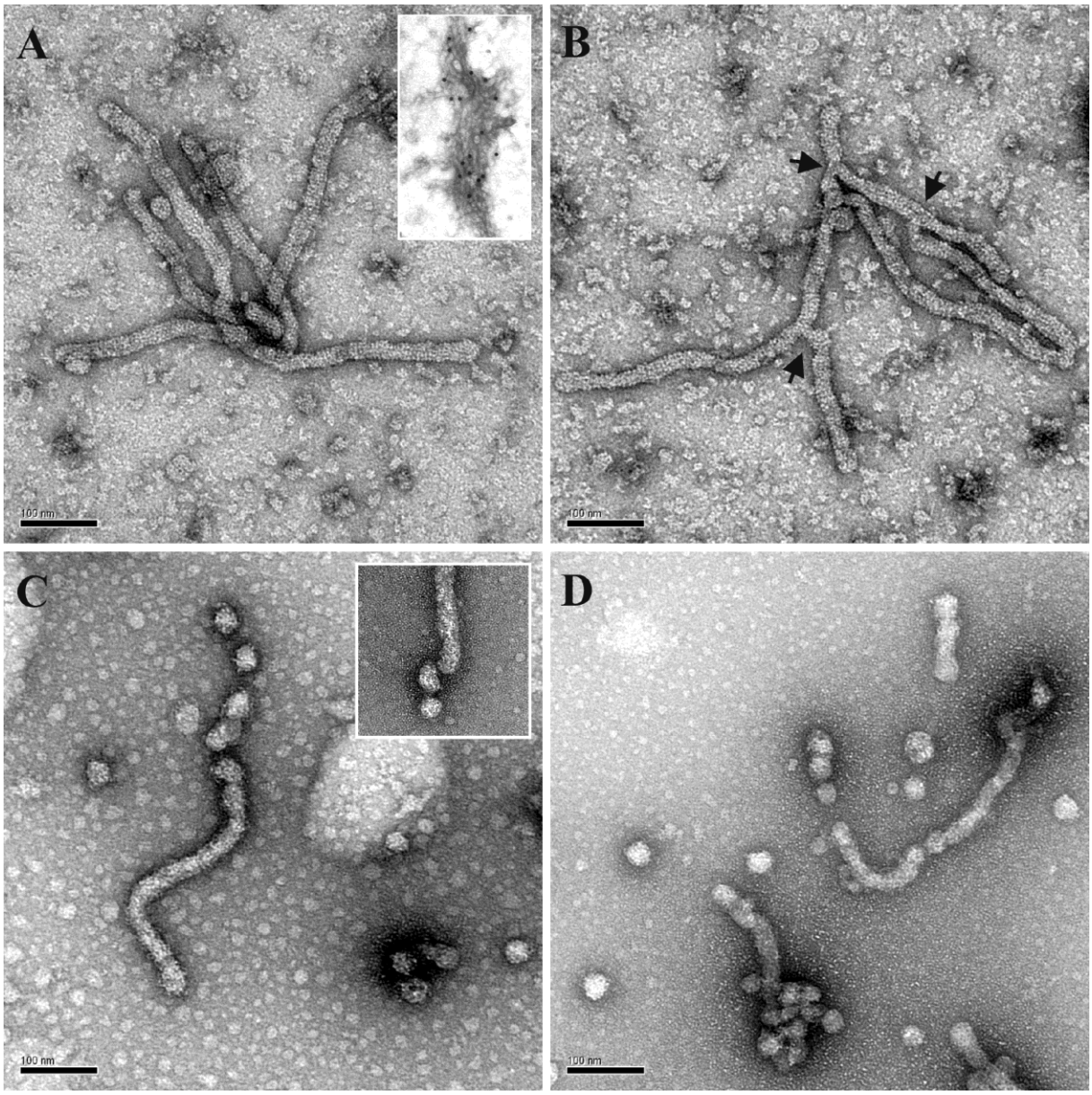

FIG. 5. Negative staining of the intracellular subviral envelope filaments purified from cells producing the HBV S protein. A first round of purification on a sucrose gradient resulted in long filaments with a diameter of 22 nm and a regular crenellated appearance (A and B), often branched (arrows in B). These filaments displayed immunoagglutination with a rabbit anti-HBs PAb and were immuno-gold labeled (inset in A). A second round of purification by affinity chromatography resulted in smaller unbranched filaments that dissociated into subviral spherical particles (C and D).

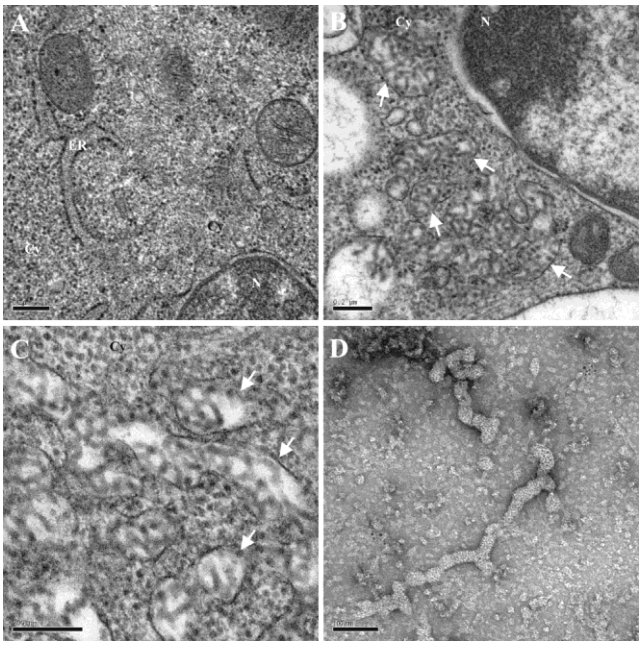

FIG. 6. EM analysis of BHK-21 cells transfected with pSFV1-MHBs^{adw} and pSFV1-LHBs^{adw}, and of HBV envelope particles recovered from these cells. No ultrastructural changes were detected in cells transfected with pSFV1-MHBs^{adw} (A), or the β-Gal construct (not shown on figures). Cells transfected with pSFV1-LHBs^{adw} showed dilated convoluted compartments containing large, branched and relaxed filamentous particles (B and C). This compartment was ER-related, as its membranes were rough and sometimes continuous with the external membrane of the nuclear envelope (white arrows). Negative staining of the filaments recovered from these cells led to the observation of small branched filaments with a diameter of 30 nm (D). Bars in A, B and C, 0.2 micrometers; Bar in D, 100 nm; N, nucleus; ER, endoplasmic reticulum; Cy, cytoplasma.